

---

# GraphFM: A Scalable Framework for Multi-Graph Pretraining

---

**Divyansha Lachi**  
Georgia Tech  
Atlanta, Georgia  
divyansha@gatech.edu

**Mehdi Azabou**  
Georgia Tech  
Atlanta, Georgia  
mazabou@gatech.edu

**Vinam Arora**  
Georgia Tech  
Atlanta, Georgia  
vinam@gatech.edu

**Eva Dyer**  
Georgia Tech  
Atlanta, Georgia  
evadyer@gatech.edu

## Abstract

Graph neural networks are typically trained on individual datasets, often requiring highly specialized models and extensive hyperparameter tuning. This dataset-specific approach arises because each graph dataset often has unique node features and diverse connectivity structures, making it difficult to build a generalist model. To address these challenges, we introduce a scalable multi-graph multi-task pretraining approach specifically tailored for node classification tasks across diverse graph datasets from different domains. Our method, Graph Foundation Model (GraphFM), leverages a Perceiver-based encoder that employs learned latent tokens to compress domain-specific features into a common latent space. This approach enhances the model’s ability to generalize across different graphs and allows for scaling across diverse data. We demonstrate the efficacy of our approach by training a model on 152 different graph datasets comprising over 7.4 million nodes and 189 million edges, establishing the first set of scaling laws for multi-graph pretraining on datasets spanning many domains (e.g., molecules, citation and product graphs). Our results show that pretraining on a diverse array of real and synthetic graphs improves the model’s adaptability and stability, while performing competitively with state-of-the-art specialist models. This work illustrates that multi-graph pretraining can significantly reduce the burden imposed by the current graph training paradigm, unlocking new capabilities for the field of graph neural networks by creating a single generalist model that performs competitively across a wide range of datasets and tasks.

## 1 Introduction

Graph neural networks (GNNs) are typically trained on individual datasets, often requiring highly specialized models [1, 2, 3] and extensive hyperparameter tuning [4]. This stems from the unique structures, sizes, and underlying concepts present in each graph, even within the same domain. As a result, an architecture optimized for one type of graph or graph problem (i.e., heterophily [5, 2], oversmoothing [6], oversquashing [1]) may not perform well on another [3]. This extreme diversity across graphs has made it challenging to build generalist models that can be applied across different types of graph data [7].

To overcome the limitations of single-graph and specialist training, there has been growing interest in building large pretrained graph foundation models [8, 9, 10]—models trained on multiple graphs

spanning different domains and tasks. However, existing approaches have been applied only to specific domains and have used relatively small amounts of training data [8]. It remains an open question whether graphs from diverse domains—ranging from molecular or protein data to product-user or recommendation graphs—can be effectively combined into a single large pretrained model.

Graph transformers offer a promising solution by enabling interactions across all nodes in a graph, treating each node and its features as a token in a sequence [11]. However, training graph transformers across many graphs is challenging due to the significant variation in graph sizes, which can range from tens to millions of nodes and edges to thousands or billions. Such high variability creates a number of bottlenecks in training, as traditional methods that rely on padding to standardize input sizes can lead to massive inefficiencies. Additionally, graphs from different domains exhibit unique structural characteristics and require the extraction of domain-specific features. For example, molecular graphs representing chemical compounds differ fundamentally from social network graphs in both structure and important features. This diversity necessitates a model capable of understanding and processing a wide range of graph topologies and domain-specific attributes.

To address these challenges, we introduce GraphFM, a scalable multi-graph pretraining approach specifically tailored for training across diverse graph datasets from different domains. GraphFM uses a Perceiver-based encoder [12] that employs learned latent tokens to compress domain-specific features into a common set of “virtual nodes” that can provide a shared vocabulary to embed many graphs. We introduce novel distributed training methods that allow for packing graphs and distributed sampling for load balancing across datasets of variable sizes. To decode from the latent space of the model, we build a multi-task node decoder that queries the latent space of the architecture to extract node-level information needed to solve a variety of different node classification tasks. Collectively, our model enables training on large datasets consisting of many diverse graphs, and allows for scalable inference across distinct node classification problems.

To evaluate our approach, we conduct a number of scaling and transfer experiments on graphs spanning many domains. In total, we train GraphFM on 152 different graph datasets comprising over 7.4 million nodes and 189 million edges from diverse domains across biology (molecules, protein-protein interactions), network science (co-author citation networks), and recommendation systems (product graphs). Our pretrained models not only provide strong generalization across a wide range of different domains and types of graphs, but also provide incredibly stable finetuning performance on new tasks. This allows for rapid training on new datasets without extensive hyperparameter tuning, alleviating the burden imposed when trying to learn a specialist model from scratch. We further provide the first scaling curves for multigraph pretraining on datasets spanning many domains. Our results show that more data indeed provides benefit in transfer, and the model sizes scale in tandem with more data to provide even further improvements. This sets the stage for a paradigm shift in graph training and establishes the potentials of training on large datasets to unlock new capabilities in our processing and analysis of graph and relational data.

The main contributions of this work are as follows:

- *Development of GraphFM:* We propose a scalable approach tailored for multi-task training on diverse graphs. GraphFM is designed to leverage a wide array of graph data from diverse domains.
- *Novel graph tokenization schemes using learned latent tokens:* Our approach compresses the raw domain-specific features and position embeddings into a common latent space through cross-attention. The embeddings in our shared latent space can be considered as a form of “shared vocabulary” for graphs that can be leveraged by the model during training.
- *Scaling Analysis during Graph Pretraining:* We provide the first scaling analysis for across-domain graph training and demonstrate how pretraining larger models on a diverse range of graph types can significantly enhance the model’s ability to rapidly transfer and adapt to new datasets.

## 2 Our Approach

A core bottleneck in training large models on different graph datasets is dealing with the large variance in graph sizes (tens to millions of nodes) when training at scale. It is critical to make efficient use of computational resources when training large-scale transformers. In our case, getting this right is

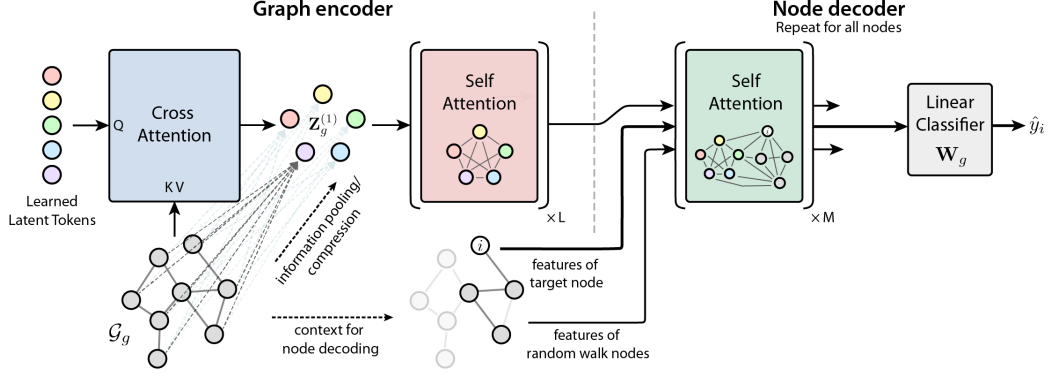


Figure 1: **Overview of GraphFM architecture and multi-graph training approach:** The input node-level tokens are passed into a cross-attention layer, and then through multiple self-attention layers. We decode node-level properties by creating a spatial sequence with features from a query node and a subset of its neighbors, which is processed through self-attention layers before being processed by a node decoder that uses self attention across the node and its neighbors.

key to making training on multiple data sources possible in the first place. Our approach achieves efficiency and scale through the following:

**1) Graph compression.** We use a Perceiver encoder to compress any input graph into a sequence of latent tokens of a fixed size using a cross-attention layer, followed by multiple self-attention layers in the latent space. Since all graphs are now represented by an equally sized sequence of latent tokens, and that most of the computation happens in the latent space, we reduce the impact of large variability in graph sizes, while significantly reducing the computational cost that is otherwise quadratic in the number of nodes.

**2) Multi-graph packing.** Typically, during batching, graphs are padded to conform to a fixed sequence length, leading to computational inefficiency, since smaller graphs require substantial padding to match the size of the largest graph in the batch. The problem is particularly pronounced when there is a significant size disparity among graphs in the same batch. To address this issue, we merge all graphs in the batch into a single large sequence of tokens, and adapt the attention mask to restrict each graph to itself. In particular, we leverage Flash Attention [13] which makes computing attention over very large sequences extremely efficient. By doing so, we avoid any superfluous padding, and this in turn improves the computational efficiency during training.

**3) Optimal Multi-GPU utilization.** Typically, maximizing GPU utilization is done by selecting a sufficiently large batch size. When training on graphs, however, we encounter two extremes: one where we can have a large batch of relatively small graphs, and another where we can only have a batch with one or two very large graphs. This means that we would be forced to lower the batch size, to avoid going out of memory when multiple large graphs are batched together. To address this issue, we developed a distributed sampler that we call *Distributed Snake Strategy Sampler* (DistributedSSSampler), which efficiently distributes graphs across multiple GPUs, and achieves high average GPU utilization across all nodes, while allowing for larger batch sizes.

## 2.1 Compressing graphs into the same latent space using a Perceiver Encoder

Each graph is represented as a sequence of node-level tokens, where each token embedding encodes both the node features and a positional embedding of the node. Let  $\mathcal{D} = \{\mathcal{G}_g\}_{g=1}^G$  denote a dataset containing  $G$  graphs, where each graph can be expressed in terms of its node and edges as  $\mathcal{G}_g = (V_g, E_g)$ , with node features  $\{\mathbf{u}_i\}_{i=1}^{N_g}$ . To process a graph with a transformer, we start by building a sequence of tokens as  $\mathbf{X}_g = [\mathbf{x}_1, \dots, \mathbf{x}_{N_g}]$ , where  $\mathbf{x}_i$  encodes both a projection of the node features using a Multi Layer Perceptron (MLP),  $\tilde{\mathbf{u}}_i = \text{MLP}_g(\mathbf{u}_i)$ , and the positional encoding (PE),  $\mathbf{p}_i$ , of the  $i^{\text{th}}$  node.

We use SignNet [14] which computes sign-invariant eigenvectors of the graph Laplacian and uses this as a basis for alignment of PE tokens across all the graphs.

To build a model that can be trained across diverse graphs, we propose to compress the graph into a fixed and common latent space. We can think about this as a way of routing communication between

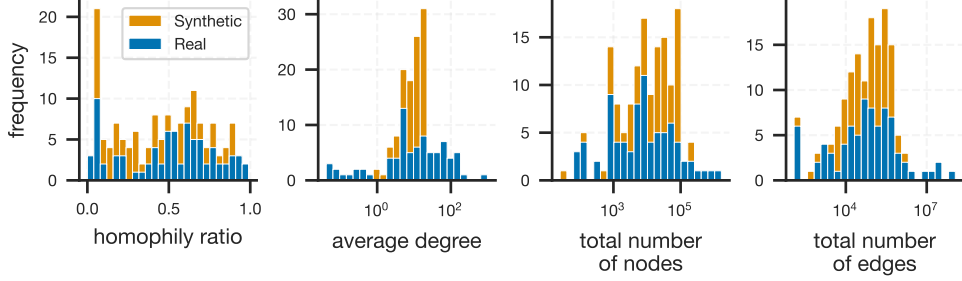


Figure 2: **Characteristics of graph datasets used to train GraphFM:** From left to right, we compute the histograms of the homophily ratio, average degree, number of nodes and number of edges of all 152 graphs used during training.

distant nodes by first going through a small number of learnable “virtual nodes” (Figure 1) that are compressed from the input graph. In particular, we leverage the Perceiver encoder [15] which has been used with images and audio to compress large sequences of input tokens into a smaller sequence of latent tokens.

For all graphs, we maintain a shared sequence of  $K$  learned latent tokens  $\mathbf{Z}_0 = [\mathbf{z}_{0,1}, \dots, \mathbf{z}_{0,K}]$ , with  $\mathbf{z}_{0,i} \in \mathbb{R}^D$  and  $K$  considerably smaller than the size of most graphs, in this work  $K = 512$ . Node embeddings in the input graph are then compressed via a cross-attention operation:

$$\mathbf{Z}_g^{(1)} \leftarrow \text{Cross-Attn}(\mathbf{Q}_g, \mathbf{K}_g, \mathbf{V}_g) = \text{softmax}\left(\frac{\mathbf{Q}\mathbf{K}_g^T}{\sqrt{d_k}}\right) \mathbf{V}_g, \quad (1)$$

where the queries,  $\mathbf{Q} = \mathbf{W}_q \mathbf{Z}_0$ , are projections of the learnable virtual node tokens, while the keys and values are projections of the graph’s token embeddings:  $\mathbf{K}_g = \mathbf{W}_k \mathbf{X}_g$  and  $\mathbf{V}_g = \mathbf{W}_v \mathbf{X}_g$ , where the key and value weight matrices are shared by all the graphs. This operation is followed by a series of  $L$  self-attention blocks in the latent space to obtain a sequence of  $K$  latent tokens,  $\mathbf{Z}_g^{\text{out}}$ .

We use the standard transformer block with pre-normalization layers and feed-forward nets. Note that the complexity here is  $KN_g + LK^2 \ll N_g^2$ ; When the number of latent tokens  $K \ll N_g$ , this results in a significant reduction in compute and memory.

*Remark.* Compressing every graph into a fixed set of virtual node embeddings, allows us to build a learnable “shared vocabulary” across graphs, and leverage common semantic and topological patterns across datasets and domains. Additionally, this approach also allows us to better integrate graphs of variable sizes, since most of the computation happens in the self-attention blocks, where all graphs are represented by an equally sized sequence of latent tokens.

## 2.2 Node decoder and multi-task learning objective

Our encoder model is designed to do the bulk of the computation when processing the graph. To be able to readout node-level features, we developed a lightweight node decoder that combines the virtual node embeddings learned by our encoder  $\mathbf{Z}_g^{\text{out}}$  with local information from a node and its neighbors to create a sequence  $\mathbf{S}_g^i$  that can be processed by a transformer to produce a final node-level estimate of its class information.

The sequence  $\mathbf{S}_g^i$  for the  $i$ th node can be represented as:

$$\mathbf{S}_g^i = \left[ \underbrace{(\mathbf{x}_i; \tau_{\text{self}})}_{\text{node}}, \underbrace{(\mathbf{x}_{\mathcal{N}_i^1}; \tau_{\text{neighbor}}) \dots (\mathbf{x}_{\mathcal{N}_i^T}; \tau_{\text{neighbor}})}_{\text{neighbors}}, \underbrace{(\mathbf{Z}_1^{\text{out}}; \tau_{\text{latent}}) \dots (\mathbf{Z}_K^{\text{out}}; \tau_{\text{latent}})}_{\text{virtual latent nodes}} \right], \quad (2)$$

where  $\mathbf{x}$  and  $\tau_{\text{type}}$  denote the features and their token type (latent, self, or neighbor), respectively, and  $\mathcal{N}_i^j$  denotes the  $j^{\text{th}}$  neighbor selected in the neighborhood of node  $i$ .

We use a small encoder-only transformer with a depth of  $M$  to obtain a final set of embeddings  $\mathbf{S}_g^{\text{out}i}$  for node  $i$ . Note that the complexity is  $M(K + T + 1)^2 \ll N_g^2$ . In the end, a per-graph linear

classifier (or regressor)  $W_g$  is tasked with producing the final predictions  $\hat{y}_i$  for node  $i$ , mapping the final embedding of node  $i$ , the first token in the  $\mathbf{S}_g^i$  sequence, to the output space as:

$\hat{y}_i = \mathbf{W}_g^T \mathbf{S}_g^{i,\text{out}}[0]$ . The linear classifier effectively translates the node-level embeddings into task-specific outputs, such as class labels for classification or continuous values for regression.

*Remark.* Since this model is trained end-to-end, the model learns how to optimally compress the graphs to maximize the performance on the various pre-training tasks. The virtual nodes allow for longer-range and more global interactions to be encoded in the virtual node embeddings, and uses this information along with the local information provided by the node’s neighbors.

**Rescaling the learning rates for different graph sizes.** When training on variable sized graphs, the MLP and linear decoder for each dataset receive updates based on the number of nodes from their respective datasets present in the batch and thus smaller graphs get updated less frequently when compared to large graphs. To mitigate this imbalance, we implemented dataset-specific learning rates for the feature MLP and linear decoders. Since they receive updates less frequently, when they do, we use a larger learning rate to update them. Without this adjustment, the weights of the common Perceiver encoder and node decoder would advance more quickly than those of the dataset-specific components, potentially leading to suboptimal learning for smaller datasets.

The details on how we set the learning rates for each pretraining dataset is provided in Section B.1 in the Appendix.

### 2.3 Balanced GPU utilization with the DistributedSSSampler

During training, the batch is formed by sampling graphs from the dataset, then splitting the batch equally among the GPUs for computation. Naively distributing small and large graphs across GPUs can lead to unbalanced GPU utilization. Our *Distributed Snake Strategy Sampler* (DistributedSSSampler) employs a bidirectional filling strategy, where graphs, sorted by their size, are distributed in a snake-like pattern, initially assigned to GPUs from right to left, then switching to left to right and so on. This method effectively pairs large graphs with small ones in subsequent passes, preventing the concentration of multiple large graphs on the same GPU, thus achieving efficient load balancing and uniform GPU utilization. A detailed algorithm and more details are provided in Appendix C.1.

We show the effectiveness of this approach in Figure 3, where we demonstrate significantly lower variance in GPU load compared to the default PyTorch batch sampler and near 100% utilization. The effectiveness is more pronounced the more GPUs are used<sup>1</sup>. This subsequently allows us to use substantially larger batch sizes, resulting in further improvement in stability and a significant 2 to 4x speed-up in training time.

## 3 Results

To evaluate our pretrained model’s capability to adapt to previously unseen data, we conducted a series of finetuning experiments on a diverse range of out-of-distribution (OOD) datasets.

### 3.1 Datasets used for pretraining and finetuning

The diversity and scale of datasets used in training our model are critical to its ability to generalize across various domains and tasks. For training, we utilize a comprehensive set of 80 real-world graph datasets, that we curated from the PyTorch Geometric library [16] and the Network Repository [17]. These datasets span a wide range of domains, graph topologies, and node features—social networks,

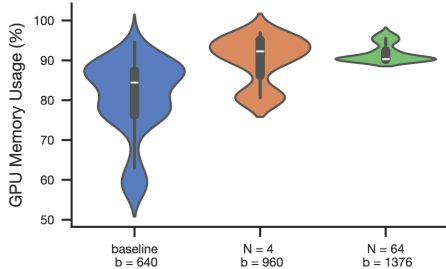


Figure 3: **Multi-GPU utilization:** GPU memory utilization during distributed training when using the default batch sampler with 8 GPUs (left) vs. our DistributedSSSampler for N=4 (middle) and N=64 (right) GPUs. The total batch size is  $N \times b$ .

<sup>1</sup>The same effect can be obtained using gradient accumulation when resource bound. See Appendix C.1

citation networks, biological protein-protein interactions, and various network infrastructures. Each dataset contributes unique structural patterns and challenges, providing a rich source for our model to learn diverse graph representations effectively.

To increase the size and diversity of our pretraining dataset even further, we include 72 synthetically generated graphs [18]. Synthetic data could be key for generating large amount of data for pre-training, and have been shown to improve the performance of large language and vision models [19, 20]. In Figure 2, we show a summary of various graph statistics, and note that the inclusion of synthetic graphs increases the density of graphs with low homophily ratio. In total, we counted more than 7.4M nodes and 163.9M edges across all datasets used for pretraining (Figure 2). We point the reader to Appendix B.1 for a detailed description of all datasets.

To demonstrate the adaptability of our pretrained model through fine-tuning on unseen data (out-of-distribution datasets), we leverage a smaller, but equally diverse set of graph datasets that are commonly used as benchmarks. We use 10 different datasets that range from academic collaboration networks like "Coauthor-CS" and "Coauthor-Physics" [21] to webpage link datasets such as "Chameleon" and "Squirrel" [22], which are particularly challenging due to their low homophily ratios, indicating less connectivity within the same class. These datasets not only test the transferability of the learned representations but also highlight the model’s capability in handling graphs with varied node degrees and class distributions.

### 3.2 Experimental Setup

**Training.** Our largest model consists of 75M parameters and is trained on 7.3M nodes (tokens). To train all of our models, we employed the LAMB optimizer [23] with a learning rate of  $10^{-4}$ . The learning rate is scheduled based on a linear warmup of 2 epochs, followed by cosine decay until the end of training. We use `bf16` mixed-precision and flash attention [13] for higher compute efficiency while training. We trained our largest model for 6.4 days on 8 NVIDIA A40 GPUs. We point the reader to further details on the architecture and model training in Appendix A and dataset-specific learning rates for the node-feature MLP and linear decoders in Table A3.

**Evaluation.** To evaluate the generalization of the pretrained model, we employed a simple fine-tuning approach for the out-of-distribution (OOD) datasets. In this setup, only the dataset-specific feature MLP at the input and the final linear decoder are updated, while the rest of the model’s parameters are kept frozen. This approach tests the model’s ability to adapt to new data with minimal additional training. For all of our fine-tuning results, we used a learning rate of  $10^{-3}$  and weight decay of  $10^{-5}$  with the AdamW optimizer [24].

**Baselines.** For the homophilic datasets we used 18 baseline model which included: 7 standard GCN-based models: GCN[25], GatedGCN [26], APPNP [27], GCNII [28], GAT[29], GATv2 [30], and superGAT [31]; 5 heterophily based models: MLP, MixHop [5], FAGCN [32], H2GCN [3] and GPRGNN [33]; 6 transformer based models: SAN [34], Graphomer [35], LiteGT[36], UniMP [37], DET[4] and NAGphormer[38]. For heterophilic datasets we compared with 14 baseline models which included: 3 standard GCN-based models: GCN, GAT, and GraphSAGE [39]; 7 heterophily-based models: MLP, HH-GCN [40], HH-GAT [40], HH-GraphSAGE [40], MixHop, GGCN [2] and H2GCN; 4 transformer based models: SAN, UniMP, DET and Gapformer [41].

### 3.3 Q1: Can we train on a lot of diverse graph datasets that span many domains?

While there has been some success in training on many graphs in the same domain [42, 8], here we wanted to ask the question of whether it is possible to train on large multi-graph datasets spanning many domains. To address this question, we trained three different sizes of models (389K, 18M, 75M) on the diverse graph datasets described in Section 3.1. We trained

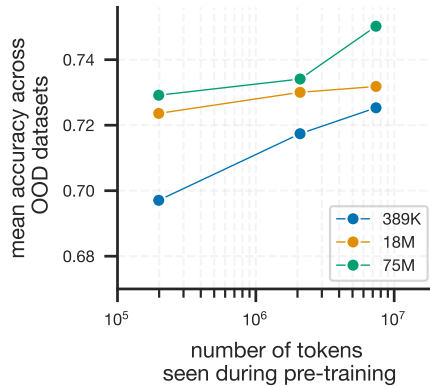


Figure 4: **Scaling analysis:** Average accuracy across OOD datasets for different model sizes (389K, 18M, 75M) and different amounts of tokens (200K, 2M, 7.3M) seen during the pre-training phase.

Table 1: *Results on node classification tasks for large graph datasets.* We report the accuracy (%) with standard deviation over 10 splits (OOM indicates Out of Memory).

Method	Photo	Physics	CS	ogbn-arxiv	Comp
<b>GCN-based methods</b>					
GCN	85.94±1.18	95.38±0.20	94.06±0.16	70.40±0.10	89.47 ± 0.46
GatedGCN	57.84±14.6	95.89±0.21	89.94±2.24	62.71±1.76	-
APPNP	84.71±1.25	95.04±0.31	87.49±0.48	70.20±0.16	90.18 ± 0.17
GCNII	67.06±1.74	94.88±0.32	84.23±0.78	69.78±0.16	-
GAT	87.13±1.00	95.14±0.28	93.61±0.14	67.56±0.12	90.78 ± 0.13
GATv2	81.52±3.23	95.02±0.32	88.46±0.61	68.84±0.13	-
SuperGAT	85.83±1.29	95.11±0.26	88.11±0.43	66.99±0.07	-
<b>Heterophily-based methods</b>					
MLP	88.66±0.85	95.12±0.26	92.99±0.51	52.63±0.12	84.63
MixHop	93.24±0.59	96.34±0.22	93.88±0.63	70.83±0.30	-
H2GCN	91.56±0.70	96.28±0.13	94.02±0.31	68.29±0.67	-
FAGCN	87.53±0.75	95.86±0.12	91.82±0.54	66.12±0.02	-
GPRGNN	92.27±0.44	96.06±0.21	93.60±0.36	68.28±0.21	89.32 ± 0.29
<b>Graph Transformer-based methods</b>					
SAN	94.17±0.65	96.83±0.18	94.16±0.36	69.17±0.15	89.83 ± 0.16
Graphormer	85.20±4.12	OOM	OOM	OOM	OOM
LiteGT	-	OOM	92.16±0.44	OOM	-
UniMP	92.49±0.47	96.82±0.13	94.20±0.34	73.19±0.18	-
DET	91.44±0.49	96.30±0.18	93.34±0.31	55.70±0.30	-
NAGphormer	94.64±0.60	96.66±0.16	95.00±0.14	-	91.22 ± 0.14
GraphFM	93.01±1.82	96.64±0.17	95.19±0.21	65.29±0.16	89.95 ± 0.83

each model on different amounts of graph data, the first with 200K tokens (small), the second with 2M tokens (medium), and then the third on 7.3M tokens (large). In all of these cases, we found that our approach could be applied successfully to solve the different multi-task objectives encountered across all the training datasets.

After pretraining, we then applied MLP finetuning to the models to a subset of the OOD datasets that included 4 homophilic (coauthor-cs, coauthor-physics, amazon-photos and amazon-comp) and 5 heterophilic (texas, wisconsin, actor, squirrel and chameleon) datasets. As hoped, we find that our performance on OOD datasets consistently improves with increasing data sizes (Figure 4). Additionally, we find that when we include all of the data (7.3M tokens) for the biggest model (75M parameters), we see a 2.1% boost in performance over the smaller model sizes. These results show clear trends that having more data and more model parameters helps in achieving better performance. Further details on the model configuration used for different sized models are provided in Appendix A.

### 3.4 Q2: How does our generalist approach compare with specialist models?

Next, we wanted to ask the question of how well our model would perform when compared with graph models that are tuned for a specific dataset. To do this, we compared the performance of our largest model (75M) with a number of message passing nets and transformer-based models. To test whether the model could indeed serve as a generalist model, we freeze the model’s weights and use the same hyperparameters (learning rate =  $10^{-3}$ ) to finetune the input and out MLPs for each new dataset. In contrast, all other models usually undergo extensive hyperparameter tuning and have dramatically different parameters across each dataset.

On both large homophilic graph datasets (Table 1) and heterophilic datasets (Table 2), we found that GraphFM was on par with state-of-the-art methods, and often outperformed other graph transformer methods trained on single datasets. Additionally, when scaling to large graphs like ogbn-arxiv and Physics, multiple graph transformer methods ran out of memory due to their use of full self-attention on all nodes in the graph. In comparison, GraphFM benefits from the reduced memory that stems from our use of the Perceiver encoder for compression. Our results demonstrate the utility of GraphFM as a scalable generalist method that doesn’t require dataset-specific architecture design or tuning.

Table 2: Results on node classification tasks for heterophilic graphs. We report the test accuracy across many heterophilic graph benchmark datasets. The standard deviation is reported across 10 train/test splits.

Method	Texas	Wisconsin	Actor	Squirrel	Chameleon
<b>GCN-based methods</b>					
GCN	55.14 ± 5.16	51.76 ± 3.06	27.32 ± 1.10	31.52 ± 0.71	38.44 ± 1.92
GAT	52.16 ± 6.63	49.41 ± 4.09	27.44 ± 0.89	36.77 ± 1.68	48.36 ± 1.58
GraphSAGE	82.43 ± 6.14	81.18 ± 5.56	34.23 ± 0.99	41.61 ± 0.74	58.73 ± 1.68
<b>Heterophily-based methods</b>					
MLP	80.81 ± 4.75	85.29 ± 3.31	36.63 ± 0.70	28.77 ± 1.56	46.21 ± 2.99
HH-GCN	71.89 ± 3.46	79.80 ± 4.30	35.12 ± 1.06	47.19 ± 1.21	60.24 ± 1.93
HH-GAT	80.54 ± 4.80	83.53 ± 3.84	36.70 ± 0.92	46.35 ± 1.86	61.12 ± 1.83
HH-GraphSAGE	85.95 ± 6.42	85.88 ± 3.99	36.82 ± 0.77	45.25 ± 1.52	62.98 ± 3.35
MixHop	77.84 ± 7.73	75.88 ± 4.90	32.22 ± 2.34	43.80 ± 1.48	60.50 ± 2.53
GGCN	84.86 ± 4.55	86.86 ± 3.29	37.54 ± 1.56	55.17 ± 1.58	71.14 ± 1.84
H <sub>2</sub> GCN	84.86 ± 7.23	87.65 ± 4.98	35.70 ± 1.00	36.48 ± 1.86	60.11 ± 2.15
<b>Graph Transformer-based methods</b>					
SAN	60.17 ± 6.66	51.37 ± 3.08	27.12 ± 2.59	-	-
UniMP	73.51 ± 8.44	79.60 ± 5.41	35.15 ± 0.84	-	-
ET	56.76 ± 4.98	54.90 ± 6.56	28.94 ± 0.64	-	-
Gapformer	80.27 ± 4.01	83.53 ± 3.42	36.90 ± 0.82	-	-
GraphFM	80.54 ± 2.76	83.13 ± 2.35	36.29 ± 0.63	42.80 ± 1.54	58.64 ± 1.24

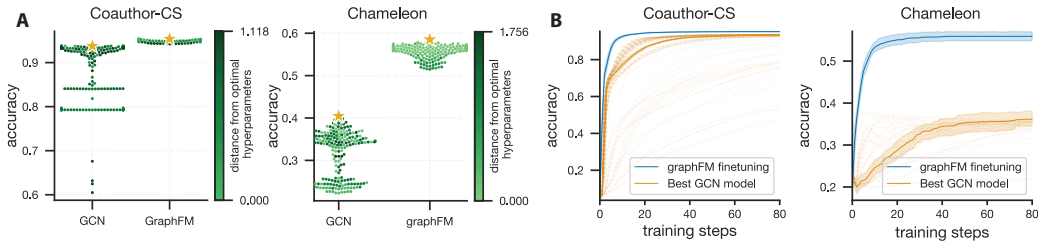


Figure 5: **Hyperparameter sensitivity and learning curves:** **A:** The performance of GCN and GraphFM for 100 different random hyperparameters on Coauthor-CS and Chameleon. The star denotes the model with the optimal hyperparameter, and the color indicates a normalized L-2 distance between the hyperparameters of each model and this optimal solution. **B:** Learning curves for 100 random GCN models and GraphFM finetuning for Coauthor-CS and Chameleon. Refer to Figure A2 for additional datasets.

### 3.5 Sensitivity to hyperparameters

In the context of graph-based models, sensitivity to hyperparameter settings and architecture is a well-documented challenge [4, 18], with many methods exhibiting significant performance variability in performance over different hyperparameters such as learning rate and depth.

To evaluate the robustness of our fine-tuned model against this common issue, we conducted an experiment that varied these critical hyperparameters within a reasonable range during the fine-tuning of our model and a standard GCN model. Our model has only two hyperparameters—learning rate and weight decay—since the model dimensions remain constant. In contrast, for the GCN model, we employed the standard random hyperparameter grid search used in [43] (see Table A4 in Appendix).

In Figure 5A, we plot the performance of both GCN and GraphFM on the Coauthor-CS and Chameleon dataset for different hyperparameters. The best model is marked with a star, and is defined by a hyperparameter vector. We color the remaining models based on the normalized distance of their hyperparameter vectors to the optimal hyperparameter vector, and note that darker green represents larger deviation from the optimal hyperparameters. For GraphFM, we observe that the distribution is concentrated around the optimal point, suggesting low sensitivity to the choice of the hyperparameters used for finetuning. We also observe that the relationship between hyperparameter deviation and performance is linear. On the other hand, for the GCN model, small deviations in hyperparameters can lead to large changes in performance, suggesting instability of the model with respect to the hyperparameters and a much noisier landscape around the optimal model.



### 3.6 Convergence speed and stability

An advantage of GraphFM is that it requires only a single fine-tuning run, significantly reducing the overall computational expense associated with hyperparameter optimization. To understand the learning dynamics and stability of finetuning, we compared the learning curves of our model during finetuning with those of a standard Graph Convolutional Network (GCN) (Figure 5B). We find that GraphFM rapidly learns and reaches asymptotic performance within 10-20 training steps, and in contrast, the GCN has much slower convergence. This quick convergence demonstrates the effectiveness of leveraging the priors from a large pretrained model. Additionally, it is important to note that most of the GCN models generated during the random hyperparameter search do not perform well. This incurs a considerable cost, since the cost of training is not only that of the final model, but of all of the models trained during hyperparameter tuning. This further highlights the advantage of using a pretrained model, which consistently provides a robust starting point that outperforms even the best GCN configuration.

## 4 Related Work

**Scaling up graph transformers.** Graph transformers bypass standard local learning rules in GNNs by allowing all nodes on the graph to interact through self-attention [44]. However, due to the high computational cost and benefits of the inductive bias in message passing, a number of methods have been proposed to move beyond full self-attention or combine transformers with GNNs. One class of methods combine transformer blocks with GNNs, including GraphTrans [45], GraphGPS [46], and SAT [47]. Another strategy is to reduce the computational complexity by using the transformer module on a coarsened or compressed graph. For instance, ANS-GT [48] introduced a node-sampling-based graph transformers, incorporating hierarchical attention and graph coarsening, and Gapformer [41] uses k-hops local pooling and global pooling to coarsen the large graph into a smaller set of nodes. Exphormer [49] coarsens the graph by doing computation through expander graphs [50]. This idea of compression has also been studied through the lens of “skeletonization” [51] where they learn to identify uninformative background nodes [51] and use this information to compress them to achieve competitive performance with as little as 1% of the nodes in the graph. Many of these approaches leverage virtual nodes to facilitate message passing across large graphs, however, the compression techniques used in these works are often based on heuristics like pooling layers or expander graphs, in contrast to our work where the compression is fully learned.

**Foundation models for graphs.** Foundation models have achieved significant success for language, vision and timeseries data [52, 53, 54]. These models are pre-trained on large datasets and can be adapted to a wide range of downstream tasks, effectively utilizing both prior knowledge from the pre-training stage and data from the downstream tasks to enhance performance [55]. The development of graph foundation and generalist models for graphs, is still in its early stages [10, 42, 9], with notable work designed for a specific sub-classes of graphs, like Triplet-GMPNN [10] which is a foundational GNN for algorithmic reasoning tasks that is trained to perform various tasks from the CLRS benchmark [56], or ULTRA [9], a foundation model for knowledge graphs trained on graphs with arbitrary entity and relation vocabularies. To our knowledge, our work is the first to tackle a wide variety of domains, datasets and tasks. The challenges and promises of graph foundation models have also been discussed in the literature [8, 57]. In recent work [8], the authors advocate for a “Graph Vocabulary” akin to the token vocabulary used in language or patches used in vision. Indeed, finding common patterns across datasets is key to enabling transfer across tasks and diverse graphs, and possibly learning universal rules and patterns. Our proposed graph compression and latent token approach provides an important contribution that aims to address this problem: instead of designing the vocabulary, we train our model to learn key structures and patterns in graph data in its latent tokens. Critically, take into account not only the topology but also the semantic features of the nodes, they also can compress information at different scales, and with different receptive fields, providing us with a multi-scale representation of the graph.

## 5 Conclusion

This paper introduces a novel approach for multi-graph training called GraphFM. Our main contributions lie in developing a unified framework for graph modeling by training on a diverse array of datasets. By leveraging pretrained models, our one generalist model achieves competitive results

across a wide range of graph benchmarks, demonstrating its effectiveness and versatility. Notably, our work demonstrates good scaling properties for graph training, where the out-of-distribution performance improves with the amount and diversity of training data. This particular analysis highlights the potential of graph learning methodologies to leverage data across different domains, enabling more efficient and effective training processes.

While our approach has shown promising results across a wide range of datasets, there are still several limitations and areas for future exploration. One limitation is the current focus on node-level classification; To broaden the applicability of this method, future work can expand the types of tasks we can perform to graph-level classification tasks, link prediction and even self-supervised learning tasks. An interesting direction is to continue expanding the diversity of datasets used for pretraining, to include point clouds and mesh graphs, knowledge graphs and even images. Moving forward, we anticipate that graph foundation models can have major impact on many facets of society, with pretraining helping to accelerate progress in new domains where data is limited or incomplete.

## References

- [1] J. Topping, F. Di Giovanni, B. P. Chamberlain, X. Dong, and M. M. Bronstein, “Understanding over-squashing and bottlenecks on graphs via curvature,” *arXiv preprint arXiv:2111.14522*, 2021. [1](#)
- [2] Y. Yan, M. Hashemi, K. Swersky, Y. Yang, and D. Koutra, “Two sides of the same coin: Heterophily and oversmoothing in graph convolutional neural networks,” in *2022 IEEE International Conference on Data Mining (ICDM)*, pp. 1287–1292, IEEE, 2022. [1](#), [6](#)
- [3] J. Zhu, Y. Yan, L. Zhao, M. Heimann, L. Akoglu, and D. Koutra, “Beyond homophily in graph neural networks: Current limitations and effective designs,” *Advances in neural information processing systems*, vol. 33, pp. 7793–7804, 2020. [1](#), [6](#)
- [4] L. Guo, Q. Zhang, and H. Chen, “Unleashing the power of transformer for graphs,” *arXiv preprint arXiv:2202.10581*, 2022. [1](#), [6](#), [8](#)
- [5] S. Abu-El-Haija, B. Perozzi, A. Kapoor, N. Alipourfard, K. Lerman, H. Harutyunyan, G. Ver Steeg, and A. Galstyan, “Mixhop: Higher-order graph convolutional architectures via sparsified neighborhood mixing,” in *international conference on machine learning*, pp. 21–29, PMLR, 2019. [1](#), [6](#)
- [6] N. Keriven, “Not too little, not too much: a theoretical analysis of graph (over) smoothing,” *Advances in Neural Information Processing Systems*, vol. 35, pp. 2268–2281, 2022. [1](#)
- [7] W. Hu, M. Fey, M. Zitnik, Y. Dong, H. Ren, B. Liu, M. Catasta, and J. Leskovec, “Open graph benchmark: Datasets for machine learning on graphs,” *Advances in neural information processing systems*, vol. 33, pp. 22118–22133, 2020. [1](#), [15](#)
- [8] H. Mao, Z. Chen, W. Tang, J. Zhao, Y. Ma, T. Zhao, N. Shah, M. Galkin, and J. Tang, “Graph foundation models,” 2024. [1](#), [2](#), [6](#), [9](#)
- [9] M. Galkin, X. Yuan, H. Mostafa, J. Tang, and Z. Zhu, “Towards foundation models for knowledge graph reasoning,” *arXiv preprint arXiv:2310.04562*, 2023. [1](#), [9](#)
- [10] B. Ibarz, V. Kurin, G. Papamakarios, K. Nikiforou, M. Bennani, R. Csordás, A. J. Dudzik, M. Bošnjak, A. Vitvitskyi, Y. Rubanova, A. Deac, B. Bevilacqua, Y. Ganin, C. Blundell, and P. Veličković, “A generalist neural algorithmic learner,” in *Proceedings of the First Learning on Graphs Conference (B. Rieck and R. Pascanu, eds.)*, vol. 198 of *Proceedings of Machine Learning Research*, pp. 2:1–2:23, PMLR, 09–12 Dec 2022. [1](#), [9](#)
- [11] L. Müller, M. Galkin, C. Morris, and L. Rampásek, “Attending to graph transformers,” *arXiv preprint arXiv:2302.04181*, 2023. [2](#)
- [12] A. Jaegle, F. Gimeno, A. Brock, O. Vinyals, A. Zisserman, and J. Carreira, “Perceiver: General perception with iterative attention,” in *International conference on machine learning*, pp. 4651–4664, PMLR, 2021. [2](#)
- [13] T. Dao, “Flashattention-2: Faster attention with better parallelism and work partitioning,” *arXiv preprint arXiv:2307.08691*, 2023. [3](#), [6](#)
- [14] D. Lim, J. Robinson, L. Zhao, T. Smidt, S. Sra, H. Maron, and S. Jegelka, “Sign and basis invariant networks for spectral graph representation learning,” *arXiv preprint arXiv:2202.13013*, 2022. [3](#)

- [15] A. Jaegle, S. Borgeaud, J.-B. Alayrac, C. Doersch, C. Ionescu, D. Ding, S. Koppula, D. Zoran, A. Brock, E. Shelhamer, *et al.*, “Perceiver io: A general architecture for structured inputs & outputs,” *arXiv preprint arXiv:2107.14795*, 2021. 4
- [16] M. Fey and J. E. Lenssen, “Fast graph representation learning with PyTorch Geometric,” in *ICLR Workshop on Representation Learning on Graphs and Manifolds*, 2019. 5
- [17] R. Rossi and N. Ahmed, “Networkrepository: An interactive data repository with multi-scale visual analytics,” 2014. 5
- [18] A. Tsitsulin, B. Rozemberczki, J. Palowitch, and B. Perozzi, “Synthetic graph generation to benchmark graph learning,” *arXiv preprint arXiv:2204.01376*, 2022. 6, 8
- [19] R. Liu, J. Wei, F. Liu, C. Si, Y. Zhang, J. Rao, S. Zheng, D. Peng, D. Yang, D. Zhou, *et al.*, “Best practices and lessons learned on synthetic data for language models,” *arXiv preprint arXiv:2404.07503*, 2024. 6
- [20] S. I. Nikolenko, *Synthetic data for deep learning*, vol. 174. Springer, 2021. 6
- [21] A. Sinha, Z. Shen, Y. Song, H. Ma, D. Eide, B.-J. Hsu, and K. Wang, “An overview of microsoft academic service (mas) and applications,” in *Proceedings of the 24th international conference on world wide web*, pp. 243–246, 2015. 6, 15
- [22] B. Rozemberczki, C. Allen, and R. Sarkar, “Multi-scale attributed node embedding,” *Journal of Complex Networks*, vol. 9, no. 2, p. cnab014, 2021. 6, 15
- [23] Y. You, J. Li, S. Reddi, J. Hseu, S. Kumar, S. Bhojanapalli, X. Song, J. Demmel, K. Keutzer, and C.-J. Hsieh, “Large batch optimization for deep learning: Training bert in 76 minutes,” *arXiv preprint arXiv:1904.00962*, 2019. 6
- [24] I. Loshchilov and F. Hutter, “Decoupled weight decay regularization,” *arXiv preprint arXiv:1711.05101*, 2017. 6
- [25] T. N. Kipf and M. Welling, “Semi-supervised classification with graph convolutional networks,” *arXiv preprint arXiv:1609.02907*, 2016. 6
- [26] Y. Li, D. Tarlow, M. Brockschmidt, and R. Zemel, “Gated graph sequence neural networks,” *arXiv preprint arXiv:1511.05493*, 2015. 6
- [27] J. Klicpera, A. Bojchevski, and S. Günnemann, “Combining neural networks with personalized pagerank for classification on graphs,” in *International conference on learning representations*, 2019. 6
- [28] M. Chen, Z. Wei, Z. Huang, B. Ding, and Y. Li, “Simple and deep graph convolutional networks,” in *International conference on machine learning*, pp. 1725–1735, PMLR, 2020. 6
- [29] P. Velickovic, G. Cucurull, A. Casanova, A. Romero, P. Lio, Y. Bengio, *et al.*, “Graph attention networks,” *stat*, vol. 1050, no. 20, pp. 10–48550, 2017. 6
- [30] S. Brody, U. Alon, and E. Yahav, “How attentive are graph attention networks?,” *arXiv preprint arXiv:2105.14491*, 2021. 6
- [31] D. Kim and A. Oh, “How to find your friendly neighborhood: Graph attention design with self-supervision,” *arXiv preprint arXiv:2204.04879*, 2022. 6
- [32] D. Bo, X. Wang, C. Shi, and H. Shen, “Beyond low-frequency information in graph convolutional networks,” in *Proceedings of the AAAI conference on artificial intelligence*, vol. 35, pp. 3950–3957, 2021. 6
- [33] E. Chien, J. Peng, P. Li, and O. Milenkovic, “Adaptive universal generalized pagerank graph neural network,” *arXiv preprint arXiv:2006.07988*, 2020. 6
- [34] D. Kreuzer, D. Beaini, W. Hamilton, V. Létourneau, and P. Tossou, “Rethinking graph transformers with spectral attention,” *Advances in Neural Information Processing Systems*, vol. 34, pp. 21618–21629, 2021. 6
- [35] C. Ying, T. Cai, S. Luo, S. Zheng, G. Ke, D. He, Y. Shen, and T.-Y. Liu, “Do transformers really perform badly for graph representation?,” *Advances in Neural Information Processing Systems*, vol. 34, pp. 28877–28888, 2021. 6
- [36] C. Chen, C. Tao, and N. Wong, “Litegt: Efficient and lightweight graph transformers,” in *Proceedings of the 30th ACM International Conference on Information & Knowledge Management*, pp. 161–170, 2021. 6

- [37] Y. Shi, Z. Huang, S. Feng, H. Zhong, W. Wang, and Y. Sun, “Masked label prediction: Unified message passing model for semi-supervised classification,” *arXiv preprint arXiv:2009.03509*, 2020. [6](#)
- [38] J. Chen, K. Gao, G. Li, and K. He, “Nagphormer: A tokenized graph transformer for node classification in large graphs,” *arXiv preprint arXiv:2206.04910*, 2022. [6](#)
- [39] N. K. Ahmed, R. A. Rossi, R. Zhou, J. B. Lee, X. Kong, T. L. Willke, and H. Eldardiry, “Inductive representation learning in large attributed graphs,” *arXiv preprint arXiv:1710.09471*, 2017. [6](#)
- [40] M. Azabou, V. Ganesh, S. Thakoor, C.-H. Lin, L. Sathidevi, R. Liu, M. Valko, P. Veličković, and E. L. Dyer, “Half-hop: A graph upsampling approach for slowing down message passing,” in *International Conference on Machine Learning*, pp. 1341–1360, PMLR, 2023. [6](#), [15](#)
- [41] C. Liu, Y. Zhan, X. Ma, L. Ding, D. Tao, J. Wu, and W. Hu, “Gapformer: Graph transformer with graph pooling for node classification,” in *Proceedings of the 32nd International Joint Conference on Artificial Intelligence (IJCAI-23)*, pp. 2196–2205, 2023. [6](#), [9](#), [15](#)
- [42] D. Beaini, S. Huang, J. A. Cunha, G. Moisesescu-Pareja, O. Dymov, S. Maddrell-Mander, C. McLean, F. Wenkel, L. Müller, J. H. Mohamud, *et al.*, “Towards foundational models for molecular learning on large-scale multi-task datasets,” *arXiv preprint arXiv:2310.04292*, 2023. [6](#), [9](#)
- [43] H. Pei, B. Wei, K. C.-C. Chang, Y. Lei, and B. Yang, “Geom-gcn: Geometric graph convolutional networks,” *arXiv preprint arXiv:2002.05287*, 2020. [8](#), [14](#), [15](#)
- [44] V. P. Dwivedi and X. Bresson, “A generalization of transformer networks to graphs,” *arXiv preprint arXiv:2012.09699*, 2020. [9](#)
- [45] Z. Wu, P. Jain, M. Wright, A. Mirhoseini, J. E. Gonzalez, and I. Stoica, “Representing long-range context for graph neural networks with global attention,” *Advances in Neural Information Processing Systems*, vol. 34, pp. 13266–13279, 2021. [9](#)
- [46] L. Rampásek, M. Galkin, V. P. Dwivedi, A. T. Luu, G. Wolf, and D. Beaini, “Recipe for a general, powerful, scalable graph transformer,” *Advances in Neural Information Processing Systems*, vol. 35, pp. 14501–14515, 2022. [9](#)
- [47] D. Chen, L. O’Bray, and K. Borgwardt, “Structure-aware transformer for graph representation learning,” in *International Conference on Machine Learning*, pp. 3469–3489, PMLR, 2022. [9](#)
- [48] Z. Zhang, Q. Liu, Q. Hu, and C.-K. Lee, “Hierarchical graph transformer with adaptive node sampling,” *Advances in Neural Information Processing Systems*, vol. 35, pp. 21171–21183, 2022. [9](#)
- [49] H. Shirzad, A. Velingker, B. Venkatachalam, D. J. Sutherland, and A. K. Sinop, “Expformer: Sparse transformers for graphs,” in *International Conference on Machine Learning*, pp. 31613–31632, PMLR, 2023. [9](#)
- [50] A. Deac, M. Lackenby, and P. Veličković, “Expander graph propagation,” in *NeurIPS 2022 Workshop on Symmetry and Geometry in Neural Representations*, 2022. [9](#)
- [51] L. Cao, H. Deng, Y. Yang, C. Wang, and L. Chen, “Graph-skeleton: 1% nodes are sufficient to represent billion-scale graph,” in *Proceedings of the ACM on Web Conference 2024*, WWW ’24, p. 570–581, 2024. [9](#)
- [52] A. Radford, K. Narasimhan, T. Salimans, I. Sutskever, *et al.*, “Improving language understanding by generative pre-training,” 2018. [9](#)
- [53] M. Dehghani, J. Djolonga, B. Mustafa, P. Padlewski, J. Heek, J. Gilmer, A. P. Steiner, M. Caron, R. Geirhos, I. Alabdulmohsin, R. Jenatton, L. Beyer, M. Tschannen, A. Arnab, X. Wang, C. Riquelme Ruiz, M. Minderer, J. Puigcerver, U. Evci, M. Kumar, S. V. Steenkiste, G. F. Elsayed, A. Mahendran, F. Yu, A. Oliver, F. Huot, J. Bastings, M. Collier, A. A. Gritsenko, V. Birodkar, C. N. Vasconcelos, Y. Tay, T. Mensink, A. Kolesnikov, F. Pavetic, D. Tran, T. Kipf, M. Lucic, X. Zhai, D. Keysers, J. J. Harmsen, and N. Houlsby, “Scaling vision transformers to 22 billion parameters,” in *Proceedings of the 40th International Conference on Machine Learning* (A. Krause, E. Brunskill, K. Cho, B. Engelhardt, S. Sabato, and J. Scarlett, eds.), vol. 202 of *Proceedings of Machine Learning Research*, pp. 7480–7512, PMLR, 23–29 Jul 2023. [9](#)

- [54] A. Das, W. Kong, R. Sen, and Y. Zhou, “A decoder-only foundation model for time-series forecasting,” *arXiv preprint arXiv:2310.10688*, 2023. 9
- [55] T. Brown, B. Mann, N. Ryder, M. Subbiah, J. D. Kaplan, P. Dhariwal, A. Neelakantan, P. Shyam, G. Sastry, A. Askell, *et al.*, “Language models are few-shot learners,” *Advances in neural information processing systems*, vol. 33, pp. 1877–1901, 2020. 9
- [56] P. Veličković, A. P. Badia, D. Budden, R. Pascanu, A. Banino, M. Dashevskiy, R. Hadsell, and C. Blundell, “The clsr algorithmic reasoning benchmark,” *arXiv preprint arXiv:2205.15659*, 2022. 9
- [57] J. Liu, C. Yang, Z. Lu, J. Chen, Y. Li, M. Zhang, T. Bai, Y. Fang, L. Sun, P. S. Yu, *et al.*, “Towards graph foundation models: A survey and beyond,” *arXiv preprint arXiv:2310.11829*, 2023. 9
- [58] B. Lefaudeux, F. Massa, D. Liskovich, W. Xiong, V. Caggiano, S. Naren, M. Xu, J. Hu, M. Tintore, S. Zhang, P. Labatut, D. Haziza, L. Wehrstedt, J. Reizenstein, and G. Sizov, “xformers: A modular and hackable transformer modelling library.” <https://github.com/facebookresearch/xformers>, 2022. 14
- [59] J. Palowitch, A. Tsitsulin, B. Mayer, and B. Perozzi, “Graphworld: Fake graphs bring real insights for gnns,” in *Proceedings of the 28th ACM SIGKDD Conference on Knowledge Discovery and Data Mining*, pp. 3691–3701, 2022. 14
- [60] P. W. Holland, K. B. Laskey, and S. Leinhardt, “Stochastic blockmodels: First steps,” *Social networks*, vol. 5, no. 2, pp. 109–137, 1983. 14
- [61] J. McAuley, C. Targett, Q. Shi, and A. Van Den Hengel, “Image-based recommendations on styles and substitutes,” in *Proceedings of the 38th international ACM SIGIR conference on research and development in information retrieval*, pp. 43–52, 2015. 15
- [62] Y. Luo, G. Luo, K. Yan, and A. Chen, “Inferring from references with differences for semi-supervised node classification on graphs,” *Mathematics*, vol. 10, no. 8, p. 1262, 2022. 15
- [63] V. T. Hoang, O. Lee, *et al.*, “Mitigating degree biases in message passing mechanism by utilizing community structures,” *arXiv preprint arXiv:2312.16788*, 2023. 15
- [64] H. Zeng, H. Zhou, A. Srivastava, R. Kannan, and V. Prasanna, “Graphsaint: Graph sampling based inductive learning method,” *arXiv preprint arXiv:1907.04931*, 2019. 17

## Appendix

### A Model Configuration Details

We used pretrained 3 configuration of models—small (398K), medium (18M) and large (75M)—for our analysis. Details of the configuration for each model are given in Table A1. In the first cross-attention layer, we used flash attention, whereas for all subsequent attention layers, we used memory-efficient attention. Both implementations were sourced from the xFormers library [58].

Table A1: Architectural details of GraphFM for different parameter sizes used in Section 3.3

Parameter Count	75M	18M	389K
<b>Num Latents (<math>K</math>)</b>	512	256	32
<b>Latent Dimension</b>	512	256	32
<b>Cross-Attention</b>			
Heads	4	4	4
FFN hidden dim	2048	1024	128
<b>Self-Attention</b>			
Depth ( $L$ )	12	10	4
Heads	8	4	4
FFN hidden dim	2048	1024	128
<b>Node Decoder</b>			
Depth ( $M$ )	4	4	2
Heads	8	4	4
FFN hidden dim	2048	1024	128

### B Details on pretraining and evaluation across different datasets

#### B.1 Pretraining datasets

The largest model (75M parameters) was trained on 80 real world and 72 synthetic datasets. The real world datasets and their characteristics are given in Table A3.

The synthetic datasets were created using the GraphWorld [59] using the Stochastic Block Model [60]. The generator parameters are listed in Table A2.

The small and medium datasets, as discussed in Section 3.3, were created by taking a random subset of the large dataset(80 real and 72 synthetic).

**Rescaling learning rates for different graph sizes:** The dataset-specific learning rates mentioned in Section 2.2 were heuristically determined based on the number of nodes in each graph. The rationale behind this approach is to assign higher learning rates to smaller datasets, ensuring that when the model encounters these datasets, it rapidly updates the MLP and linear decoder weights.

**Homophily:** In this work, we follow the definition of *node homophily ratio* as used in [43] given by the formula:

$$\frac{1}{|\mathcal{V}|} \sum_{v \in \mathcal{V}} \frac{|\{(v, w) : w \in \mathcal{N}(v) \wedge y_v = y_w\}|}{|\mathcal{N}(v)|},$$

where  $\mathcal{V}$  denotes the set of all nodes in the graph,  $\mathcal{N}(v)$  denotes all the neighbors of an arbitrary node  $v$ , and  $y_v$  denotes the class membership of the node  $v \in \mathcal{V}$ . We classify datasets into *homophilic datasets* and *heterophilic datasets* based on the homophily score: datasets with homophily  $\geq 0.5$  are classified as *homophilic datasets* and *heterophilic datasets* otherwise.

Table A2: Graphworld generator parameters for synthetic graphs

Parameter Name	Description	Values
nvertex	Number of vertices in the graph.	[32, 500000]
$p/q$ ratio	The ratio of in-cluster edge probability to out-cluster edge probability.	[0.1, 10.0]
avg. degree	The average expected degrees of the nodes.	[1.0, 20.0]
feature center distance	The variance of feature cluster centers, generated from a multivariate Normal.	[0.0, 5.0]
num clusters	The number of unique node labels.	[2, 6]
cluster size slope	The slope of cluster sizes when index-ordered by size.	[0.0, 0.5]
power exponent	The value of the power law exponent used to generate expected node degrees.	[0.5, 1.0]

## B.2 Fine-Tuning details

### B.2.1 Homophilic Datasets

We use five real-world datasets, Amazon Computers and Amazon Photos [61], Coauthor CS and Coauthor Physics [21] and Obgn-Arxiv [7]. Key statistics for the different datasets are listed in Table A3 in the finetuning-section. The experimental setup follows that of [62], where we split the dataset into development and test sets. All the hyperparameter tuning is done on the development set and the best models are evaluated on the test set. The runs are averaged over 20 random splits to minimize noise. We follow a 60:20:20% train/val/test split for the Amazon and Coauthor datasets. For Obgn-Arxiv we follow the experimental setup used in [7]. The results for the Coauthor-Physics, Coauthor-CS, and Amazon-Photos obtained from in Table 1 have been sourced from [41]. The results for the Amazon-Comp dataset are taken from [63] except for MLP which was obtained from [62].

### B.2.2 Heterophilic Datasets

We use five real-world datasets with graphs that have a homophily level  $\leq 0.30$ , Texas, Wisconsin and Actor [43] and Chameleon and Squirrel [22]. Key statistics for the different datasets are listed in Table A3 in the finetuning-section. We follow the experimental setup in [43], and use the same 10 train/val/test splits that are provided. The results for GCN based methods and heterophily based methods in Table 2 have been taken from [40], and the results for transformer based methods have been taken from [41]

## C Multi-Graph Training

### C.1 DistributedSSSampler

In designing this sampler, we prioritized ensuring that it neither introduces bias into the data sampling process nor alters the distribution of the graphs from the datasets. Its primary function is to enhance batch construction and distribution across GPUs.

First, the sampler defines a set of  $N$  buckets with a fixed node budget  $B$ , where  $N$  can be the number of GPUs and  $B$  is the node-level batch size. The graphs (across all GPUs) are sorted in descending order based upon their size. The sampler then employs a bidirectional filling strategy within the buckets. The distribution process, as described in Algorithm 1 involves distributing graphs in a snake-like pattern, initially filling from right to left, then switching to left to right and so on. When a graph is added to a bucket, it uses up part of the budget, equal to its size. This method effectively pairs larger graphs with smaller ones in subsequent passes, preventing the concentration of multiple

Table A3: Datasets and their characteristics

	Dataset	Number of Graphs	Nodes	Edges	Homophily Ratio	Average Degree	Node Features	Node Classes	Learning Rate
Pre-Training	BA-1_10_60-L5	1	804	46410	0.2	115.45	1	5	0.0014
	BA-2_24_60-L2	1	10693	639750	0.5	119.66	1	2	0.0087
	BZR	405	35.75	76.71	0.42	0.07	1	53	0.0082
	CL-100K-1d8-L9	1	92482	373989	0.11	8.09	1	9	0.00064
	CL-10K-1d8-L5	1	10000	44896	0.2	8.98	1	5	0.00096
	DD	1178	284.32	1431.32	0.07	0.058	1	89	0.00085
	DD199	1	841	1902	0.067	4.52	1	20	0.00085
	DD21	1	5748	14267	0.07	4.96	1	40	0.00085
	DD242	1	1284	3303	0.08	5.14	1	20	0.00042
	DD244	1	291	822	0.074	5.65	1	20	0.00085
	DD349	1	897	2087	0.05	4.65	1	20	0.00085
	DD497	1	903	2453	0.06	5.43	1	20	0.0028
	DD6	1	4152	10320	0.07	4.97	1	20	0.00085
	DD68	1	775	2093	0.072	5.4	1	20	0.0028
	DD687	1	725	2600	0.06	7.17	1	20	0.0028
	DHFR	756	42.43	89.09	0.32	0.04	3	53	0.0018
	ENZYMES	600	32.63	124.27	0.67	0.09	18	3	0.0020
	ENZYMES118	1	96	121	0.58	2.52	1	2	0.00087
	ENZYMES123	1	90	127	0.52	2.82	1	2	0.0076
	ENZYMES295	1	124	139	0.71	2.24	1	2	0.0076
	ENZYMES296	1	126	141	0.72	2.24	1	2	0.00087
	ENZYMES297	1	122	149	0.65	2.44	1	2	0.0020
	ENZYMES8	1	88	133	0.77	3.02	1	2	0.0076
	ER-AvgDeg10-100K-L2	1	99997	499332	0.50	9.99	2	2	0.0049
	ER-AvgDeg10-100K-L5	1	99997	499332	0.20	9.99	1	5	0.0013
	KKI	83	26.96	96.84	0	0.39	1	189	0.0012
	MSRC-21	563	77.52	396.65	0.74	0.13	1	24	0.0063
	MSRC-21C	209	40.28	193.20	0.61	0.27	1	10	0.0017
	MSRC-9	221	40.58	193.21	0.69	0.26	1	10	0.009
	OHSU	79	82.01	399.32	0	0.56	1	189	0.0095
	PLC-40-30-L5	1	11025	437979	0.2	79.45	1	5	0.0086
	PLC-60-30-L2	1	117572	7045181	0.5	119.84	1	2	0.0013
	PROTEINS-full	1113	39.06	145.63	0.97	0.05	2	8	0.0063
	Peking-1	85	39.31	154.71	0	0.44	1	189	0.0027
	SW-10000-6-0d3-L2	1	10000	30000	0.5	6	1	2	0.00096
	SW-10000-6-0d3-L5	1	10000	30000	0.2	6	1	5	0.0088
	SYNTHETIC	300	100	392	0.18	0.16	1	8	0.0018
	TerroristRel	1	881	8592	0.92	19.51	1	2	0.0033
	Tox21_p53	1	153563	314046	0.62	4.09	1	46	0.00054
	fb-CMU-Carnegie49	1	6637	249967	0.5	75.33	1	3	0.0010
	gene	1	1103	1672	0.4	3.03	1	2	0.012
	proteins-all	1	43471	162088	0.66	7.46	1	3	0.00075
	reality-call	1	27058	51200	0.9	15	1	1	0.0071
	Reddit	1	232965	114615892	0.76	983.98	602	41	0.0035
	Reddit2	1	232965	23213838	0.78	199.29	602	41	0.0035
	Flickr	1	89250	899756	0.31	20.16	500	7	0.0051
	Yelp	1	716847	13954819	-	38.93	300	100 <sup>1</sup>	0.00031
	Wiki	1	2405	17981	0.71	14.95	4973	17	0.0012
	BlogCatalog	1	5196	17981	0.40	132.21	8189	6	0.0099
	PPI	1	56944	1612348	0.63	56.63	50	121	0.0016
	Facebook	1	4039	88234	0.99	43.69	1283	193	0.0011
	Roman-empire	1	22662	65854	0.05	5.81	300	18	0.0074
	Amazon-ratings	1	24492	186100	0.38	15.2	300	5	0.00082
	Minesweeper	1	10000	78804	0.68	15.76	7	2	0.0088
	Tolkers	1	11758	1038000	0.59	176.56	10	2	0.0022
	Questions	1	48921	307080	0.84	12.55	301	2	0.0061
	Twitch-DE	1	9498	315774	0.64	66.49	128	2	0.0023
	Twitch-EN	1	7126	77774	0.59	21.82	128	2	0.0010
	Twitch-ES	1	4648	123412	0.59	53.10	128	2	0.0011
	Twitch-FR	1	6551	231883	0.54	70.79	128	2	0.0010
	Twitch-PT	1	1912	64510	0.58	67.47	128	2	0.0012
	Twitch-RU	1	4385	78993	0.63	36.02	128	2	0.0011
	DeezerEurope	1	28281	185504	0.52	13.11	128	2	0.0070
	GitHub	1	37700	578006	0.84	30.66	128	2	0.0065
	FacebookPagePage	1	22470	342004	0.88	30.44	128	2	0.00085
	LastFMAsia	1	7624	55612	0.87	14.59	128	18	0.0092
	Airports-Brazil	1	131	1074	0.46	16.39	131	4	0.0013
	Airports-Europe	1	399	5995	0.40	30.05	399	4	0.0015
	Airports-USA	1	1190	13599	0.69	22.85	1190	4	0.0092
	PolBlogs	1	1490	19025	0.91	25.54	1	2	0.0013
	EmailEUCore	1	1005	25571	0.36	50.89	1	42	0.0032
	penn94	1	41554	2724458	0.51	131.11	4814	2	0.0064
	reed98	1	962	37624	0.52	78.22	745	2	0.0032
	amherst41	1	2235	181908	0.53	162.78	1193	2	0.011
	johnshopkins55	1	5180	373172	0.55	144.08	2406	2	0.0025
	genius	1	421961	984979	0.62	4.67	12	2	0.00040
	CitationFull-CiteSeer	1	4230	10674	0.95	5.04	602	6	0.0011
	CitationFull-Cora-ML	1	2995	16316	0.78	10.89	2879	7	0.0028
CitationFull-PubMed	1	19717	88648	0.80	8.99	500	3	0.00087	
soc-pokec	1	1632803	30622564	0.44	37.51	500	3	0.00019	
Fine-tuning	Actor	1	7600	30019	0.21	7.89	932	5	0.001
	Amazon-Computers	1	13752	4491722	0.77	71.51	767	10	0.001
	Amazon-Photo	1	7650	238162	0.82	62.26	745	8	0.001
	Coauthor-CS	1	18333	163788	0.80	17.86	6805	15	0.001
	Coauthor-Physics	1	34493	495924	0.93	28.75	8415	5	0.001
	Chameleon	1	2277	36101	0.23	31.70	2325	5	0.001
	Obgn-Arvix	1	169343	1166243	0.65	13.77	128	40	0.001
	Squirrel	1	5201	217073	0.22	83.47	8415	5	0.001
	Texas	1	183	325	0.10	3.55	1703	5	0.001
	Wisconsin	1	251	515	0.19	4.10	1703	5	0.001

<sup>1</sup> Multi label binary classification.



Table A4: Hyperparameter Search Space

Hyperparameter	Type	Range
Hidden Dim	Categorical	{16, 32, 64, 128}
Depth	Categorical	{1, 2}
Dropout	Uniform	[0.0, 0.9]
Learning Rate	Log uniform	[5e-5, 5e-1]
Weight Decay	Log uniform	[1e-5, 1e-2]

large graphs on the same GPU, thus achieving efficient load balancing and uniform GPU utilization. Figure A1-A shows an overview of how the sampler distributes the graphs into buckets. We find that stability is improved with a larger number of buckets  $N$  (Figure A1-B). When the number of GPUs is fixed, we can achieve a larger  $N$  by using gradient accumulation, which artificially increases the number of buckets by a factor equal to the number of accumulation steps, without biasing the sampling process.

---

**Algorithm 1** Distribute graph nodes into virtual GPU buckets

---

```

1: input: Batch size  $B$ , Bucket count  $N$ , Graphs in the dataset  $\mathcal{G} = \{\mathcal{G}_0, \mathcal{G}_1, \dots\}$ , Subgraphs
   sampled for this minibatch  $\mathcal{G}^m = \{\mathcal{G}_0^m, \mathcal{G}_1^m, \dots\}$ 
2: precondition:  $\sum_i |\mathcal{G}_i^m| == N \times B$ 
3: initialize:
4:    $buckets \leftarrow$  array of  $N$  empty arrays # will store subgraphs in each bucket
5:    $counts \leftarrow$  array of  $N$  zeroes # will store number of nodes in each bucket
6:    $b \leftarrow 0$  # bucket index
7:    $d \leftarrow 1$  # direction
8:   Sort  $\mathcal{G}^m$  according to node-counts in  $\mathcal{G}$ , largest graph goes first
9: for all  $\mathcal{G}_i^m$  in  $\mathcal{G}^m$  do
10:  while  $|\mathcal{G}_i^m| > 0$  do
11:    if  $counts[b] < B$  then
12:      # insert a part of  $\mathcal{G}_i^m$  into bucket  $b$ 
13:       $n \leftarrow \min(|\mathcal{G}_i^m|, B - counts[b])$ 
14:       $counts[b] \leftarrow counts[b] + n$ 
15:      append first  $n$  nodes of  $\mathcal{G}_i^m$  to  $buckets[b]$ 
16:      remove first  $n$  nodes from  $\mathcal{G}_i^m$ 
17:    end if
18:    # go to the next bucket, switching direction at the boundaries
19:     $b \leftarrow b + d$ 
20:    if  $b \geq N$  or  $b < 0$  then
21:       $d \leftarrow -d$ 
22:       $b \leftarrow b + d$ 
23:    end if
24:  end while
25: end for
26: return  $buckets$ 

```

---

## C.2 GraphSAINT Random Walk Sampler

Efficient neighborhood sampling for large graphs is crucial for our node decoder, as traditional methods for k-hop neighborhood sampler often become computationally prohibitive with the increasing size and complexity of the graph data. To overcome these limitations, we have adopted the GraphSAINT Random Walk Sampler [64], specifically designed for efficient sampling in large-scale graphs.

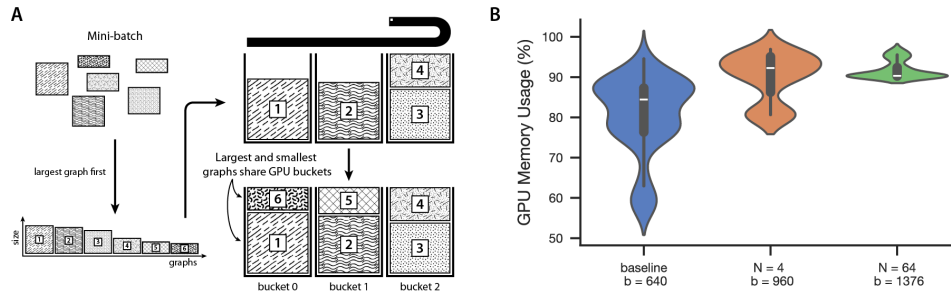


Figure A1: **Multi-GPU utilization**: **A**: A diagram visualizing our sample distribution strategy. **B**: GPU memory utilization during distributed training when using the default batch sampler vs. our DistributedSSSampler for  $N=4$  and  $N=64$  buckets.

### C.3 RAM Optimization in Multi-GPU Environments

In multi-GPU training environments, efficient use of system memory is crucial, especially when handling large graph datasets. Traditional approaches lead to substantial memory redundancy, as each GPU process typically loads a complete dataset into system RAM. This results in each process duplicating the dataset in system memory, leading to inefficient memory usage and potential system overload.

To address this, we utilize a shared memory management approach using Python's `multiprocessing.Manager()` to coordinate dataset access across multiple GPU processes. This method ensures that each dataset is loaded into RAM only once, regardless of the number of GPUs, thereby avoiding duplication and conserving memory resources.

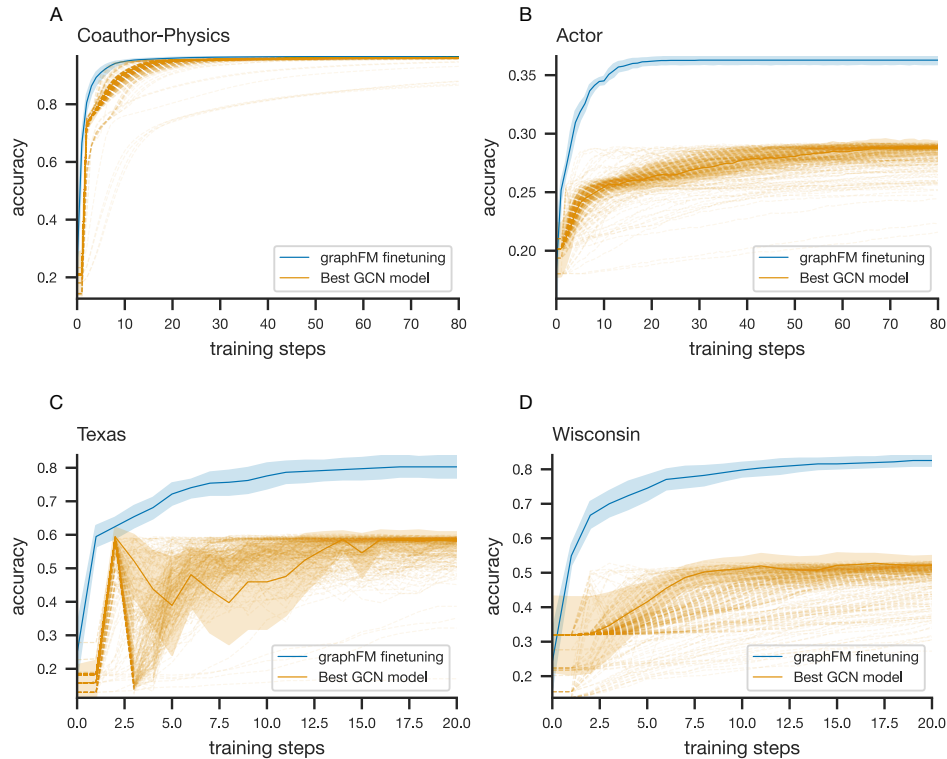


Figure A2: **Additional learning curves**: Learning curves for 100 random GCN models and GraphFM finetuning for Coauthor-Physics, Actor, Texas and Wisconsin